THE JOURNAL OF PHYSICAL CHEMISTRY B

 VOLUME 105, NUMBER 13, APRIL 5, 2001

LETTERS

FRET by FET and Dynamics of Polymer Folding

Goundla Srinivas,[†] Arun Yethiraj,[‡] and Biman Bagchi*[,†]

Solid State and Structural Chemistry Unit, Indian Institute of Science, Bangalore, India 560 012, and Department of Chemistry, University of Wisconsin, Madison, Wisconsin 53706

Received: September 18, 2000; In Final Form: February 7, 2001

Fluorescence resonance energy transfer (FRET) is a powerful tool for the investigation of the conformational and dynamic properties of macromolecules. In this work, we report Brownian dynamics simulations of FRET during polymer folding. The polymer molecule is modeled as a necklace of beads that interact via a site−site Lennard-Jones interaction, and FRET occurs via Forster energy transfer between the ends of the chain. The simulations demonstrate that FRET can act as a good marker of polymer folding only when the Forster radius (R_F) is smaller than the root-mean-square radius (R_0) of the polymer. FRET is sensitive to the early stages of polymer folding for $R_F \leq R_0$ and to the late stages of polymer folding for $R_F \ll R_0$. This suggests that it might be necessary to employ more than one donor−acceptor pair in experiments aimed at probing the entire dynamics of polymer folding.

1. Introduction

Direct investigation of the conformational dynamics of polymers and biopolymers is a long-standing and challenging experimental problem.[1−4] Recently, fluorescence resonance energy transfer (FRET) has been combined with the techniques of single molecule spectroscopy to provide a powerful tool that allows the study of structure and dynamics of polymers and biopolymers in solution.[5−8] In FRET, the polymer is doped with donor and acceptor sites at suitable positions along the chain backbone.[6,8−10] The donor is excited optically, and the energy transfer to the acceptor is monitored. The mechanism of excitation energy migration is widely believed to occur by Forster energy transfer (FET),[11] where the singlet−singlet resonance energy transfer rate $k(R)$ is given by

$$k(R) = k_F\left(\frac{R_F}{R}\right)^6 \quad (1)$$

where R_F is the Forster radius, defined as the donor−acceptor separation corresponding to the 50% of energy transfer, and k_F is the rate of excitation transfer when $R = R_F$. Both k_F and R_F are determined solely by the donor−acceptor pair. The Forster radius is usually obtained from the overlap of the donor fluorescence with the acceptor absorption and several other available parameters.[12] The strong dependence of the energy transfer rate on the donor−acceptor separation allows one to extract valuable information on the conformations of rigid biopolymers from FRET experiments.[5,6,9] In flexible molecules, the distance between donor and acceptor sites fluctuates[6,12−14] with time, and in this case, FRET experiments provide information on the conformational dynamics of macromolecules.

The quantity of primary importance in FRET experiments is the time dependent survival probability of the excitation on the donor (denoted by $S_P(t)$) which is the fraction of donors from which excitation transfer has not occurred (i.e., the donor has survived) at time t. This quantity is directly proportional to the

* To whom correspondence should be addressed. E-mail: bbagchi@sscu.iisc.ernet.in.
[†] Indian Institute of Science.
[‡] University of Wisconsin.

10.1021/jp0033723 CCC: $20.00
Published on Web 03/08/2001

time dependent fluorescence intensity (or fluorescence quantum yield) measured in FRET experiments.

In this work, we investigate FRET during the folding of a single polymer chain using Brownian dynamics (BD) simulations. For simplicity, we specify the polymer chain with the donor−acceptor pair attached to the two ends (one at each end) of the same polymer chain. Thus FRET has a strong dependence on end-to-end separation. In experiments, one monitors the time dependence of fluorescence from the donor; the donor fluorescence disappears on FET. Thus, the intensity of the fluorescence is a measure of the fraction un-reacted at time t. We calculate this survival probability $S_p(t)$.

2. Time Scales

Analysis of the results requires the understanding of *three* relevant time scales. Two time scales, $\tau_{F,fold}$ and $\tau_{F,unf}$, correspond to the average survival probability of FRET in the equilibrium folded and unfolded states, respectively. These two time scales are widely separated from each other because of the sensitivity of the survival time to the separation between the two ends. This separation between the ends is very different in the unfolded and folded states. In fact, mean square end-to-end distance scales as $N^{2\nu}$, where $\nu \approx 0.5-0.6$ in the unfolded state (depending on the solvent conditions) and $\nu \approx {}^1/_3$ in the folded state.[15,16]

The third relevant time scale in this problem is the time, $\tau_{q,fold}$, required for the polymer to fold after a quench in the temperature (or solvent quality). For FRET to be useful in the study of folding, $\tau_{q,fold}$ has to be intermediate and well-separated from the other two characteristic times, i.e.

$$\tau_{E,fold} \ll \tau_{q,fold} \ll \tau_{E,unf} \tag{2}$$

3. Simulation Details

The polymer chain is modeled as a necklace of beads that interact via a site−site Lennard-Jones potential. Neighboring beads are connected via harmonic springs. The total potential energy U is given by[17]

$$U = \sum_{i=2}^{N}\sum_{j=1}^{i-1} u_{LJ}(r_{ij}) + \sum_{i=2}^{N} u_b(|\mathbf{r}_i - \mathbf{r}_{i-1}|) \tag{3}$$

where N is the number of beads, $\mathbf{r}_i$ is the position of bead i, $r_{ij} = |\mathbf{r}_i - \mathbf{r}_j|$, and $u_{LJ}(r)$ is the Lennard-Jones potential

$$u_{LJ}(r) = \epsilon\left[\left(\frac{\sigma}{r}\right)^{12} - \left(\frac{\sigma}{r}\right)^{6}\right] \tag{4}$$

and u_b is the bonding potential

$$u_b(r) = \frac{3\kappa k_B T}{2b^2}(r-b)^2 \tag{5}$$

In the above, σ and ϵ are the Lennard-Jones collision diameter and well depth, respectively, b is the average bond length, k_B is Boltzmann's constant, T is the temperature, and κ is the stiffness of the spring. In this work, we use $\kappa = 9$, $N = 80$, and $b = \sigma$. We define the mass, length, and time scales by setting the mass of each bead m, the bond length b, and the single bead diffusion coefficient D_0 to unity. The unit of time τ is σ^2/D_0. For convenience, we define $\epsilon^* \equiv \epsilon/\kappa_B T$.

For each trajectory, an initial configuration is obtained from equilibrium Monte Carlo simulations at the required value of ϵ^*. The time evolution of the positions of the beads is governed by the following equation of motion:

$$\mathbf{r}_j(t+\Delta t) = \mathbf{r}_j(t) + \mathbf{F}_j(t)\frac{D_0}{\kappa_B T}\Delta t + \Delta \mathbf{X}^G(t) \tag{6}$$

where $\mathbf{r}_j(t)$ is the position of bead j at time t, $\mathbf{F}_j(t)$ the force on bead j due to interaction with other beads at time t, and $\Delta\mathbf{X}^G(t)$ is the stochastic Brownian force on bead j at time t. This stochastic force is selected from a Gaussian distribution with zero mean and a variance of $2\Delta t$. In the BD simulations, we use a time-step $\Delta t = 0.0005\tau$ in the unfolded state and during the folding process and $\Delta t = 0.0001\tau$ in the folded state.

The simulations proceeds as follows. An initial configuration is generated at $\epsilon^* = 0.1$, and the temperature is then instantaneously reduced to a value of $\epsilon^* = 0.8$. The positions of the beads are then propagated using BD. At each time step, the end-to-end distance R is calculated and the trajectory is terminated with probability $k(R)$ obtained from eq 1. Averages are obtained over 50 000−100 000 independent trajectories. More details on the simulation and averaging procedure can be found elsewhere.[18] In addition to the survival probability, we also monitor the time dependent total energy, root-mean-square end-to-end distance, and radius of gyration.

4. Choice of Forster Rate Parameters

FRET is capable of providing information about the folding process only for certain values of R_F which depend on the size of the folded and unfolded states. If R_F is very large, much greater than the size of the unfolded chain, then the reaction rate is very fast in both folded and unfolded states and FRET fails to serve as a dynamic marker of the folding process. If R_F is very small, much smaller than the size of the folded chain, then the reaction rate is slow enough that only the last stage of the folding process is monitored by FRET. It is therefore essential to choose a value of R_F that allows one to probe both the folded and unfolded states. For $N = 80$, the root-mean-square end-to-end distance is approximately equal to 7.3 and 3.5 in the unfolded and folded states, respectively. We investigate several combinations of R_F and k_F, and from trial and error we find that values of $R_F = 4$ and $k_F = 10$ satisfy our criterion of being able to probe both the folded as well as unfolded states.

5. Dynamics of Polymer Folding

Figure 1 depicts snapshots of a polymer at different times during the course of the BD simulation. As has been observed previously, the folding process starts from the chain ends. Initially blobs or nucleation sites are formed bridged by linear segments. These blobs grow by accumulating monomers from the bridges until they coalesce to form a compact globule.

Figure 2 depicts the survival probability $S_p(t)$ as a function of time for the folded and unfolded states. (The inset depicts $S_p(t)$ over a longer time duration.) The decay of $S_p(t)$ is roughly exponential over the entire time period in both cases. As can be seen from the figure, the time taken for two ends to react is large in the unfolded state compared to that in the folded state. In fact, the decay of $S_p(t)$ is extremely fast in the folded state, almost 3 orders of magnitude faster than the unfolded state. Clearly, our criteria, $\tau_{E,fold} \ll \tau_{E,unf}$, is satisfied.

Results for FRET during the folding process are shown in Figure 3. For comparison $S_p(t)$ for the unfolded state is also shown in the same figure. During the folding process, the survival probability initially follows the decay path of the unfolded state. For $t \geq 100\tau$, $S_p(t)$ during the folding process

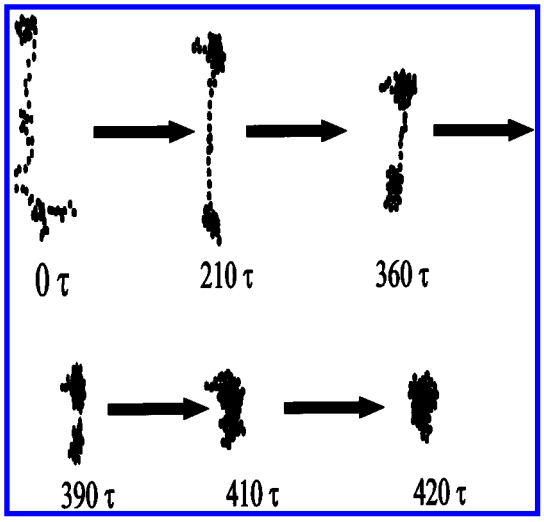

Figure 1. Snapshots of the polymer chain at various times during the folding process.

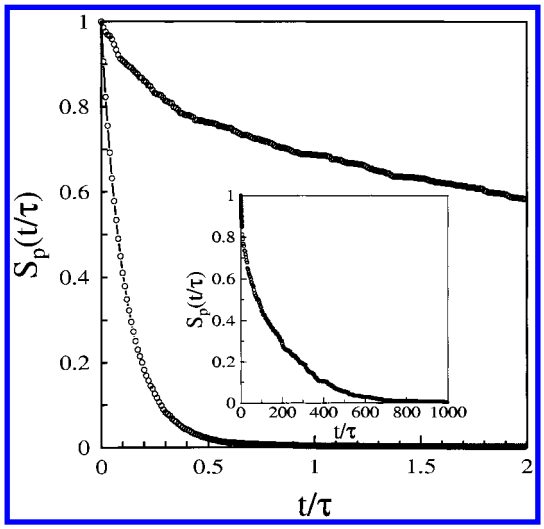

Figure 2. Survival probability $S_p(t)$ as a function of time t for equilibrium simulations of the unfolded state (upper curve) and the folded state (lower curve) which correspond to reduced inverse temperatures of $\epsilon^* = 0.1$ and 0.8, respectively. The inset depicts $S_p(t)$ for the unfolded state over a longer time duration than the main figure.

begins to deviate from the $S_p(t)$ of the unfolded chain and the decay of $S_p(t)$ becomes more rapid. In other words, the characteristic decay time of $S_p(t)$ switches from $\tau_{E,unf}$ to $\tau_{q,fold}$.

Figure 4 depicts the mean square end-to-end distance $\langle R^2 \rangle$ during the folding process. (Similar behavior is also observed for the variation of the mean-square radius of gyration with time and is therefore not shown.) For the chosen set of parameters, polymer folding occurs after approximately 100τ, which is also the time (i.e., 100τ) where the deviation in $S_p(t)$ from the unfolded configuration starts (see Figure 3). More importantly, the major part of FRET occurs within a time of 200τ, which is the average time taken for a polymer to collapse to approximately *half* of the mean square end-to-end distance of the initial unfolded configuration. The inset of Figure 4 depicts the total energy of the polymer during the folding process. The total energy of polymer chain begins to decrease immediately after the quench and continues to do so till it reaches the energy of the final configuration. Note that the total energy begins to decrease immediately after the quench, i.e., at time $t = 0$, whereas the size of the chain starts decreasing only after an initial time delay. This is because the initial decrease of energy

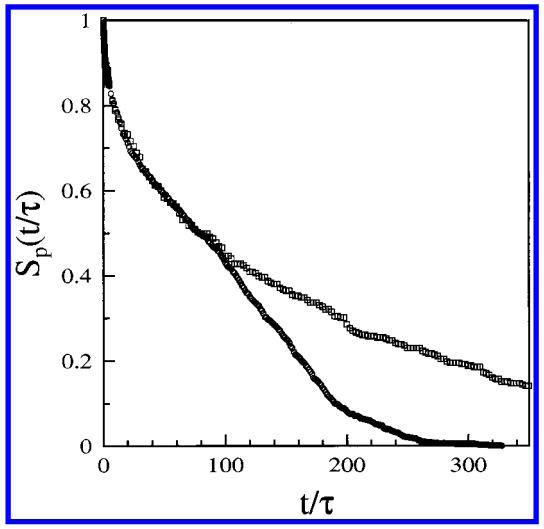

Figure 3. Survival probability for the polymer during the folding process (○, lower curve) compared to the same function for the equilibrium unfolded state (□, upper curve). For $t \approx 100\tau$, $S_p(t)$ during the folding process begins to decay considerably faster than for the unfolded polymer and has decayed essentially to zero by approximately 280τ.

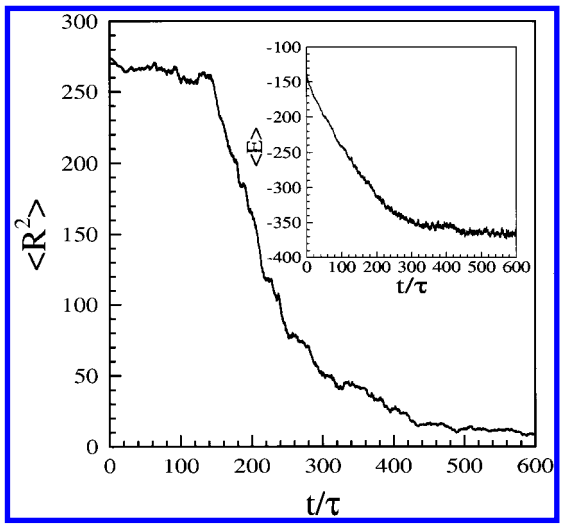

Figure 4. The mean square end-to-end distance $\langle R^2 \rangle$ and average total energy (inset) as a function of time during the folding process. There is an initial delay in the decay of $\langle R^2 \rangle$ after the quench, after which the polymer size starts decreasing. There is no such delay in the decay of the total energy.

does not require a change in the chain size; it occurs by establishing favorable contacts.

6. Conclusion

The main results of the present study are in Figures 2−4 which show the reliability of FRET as a dynamic marker in the folding process. We have carried out several other studies, including embedding the donor−acceptor pair at different locations along the chain. For example, one can efficiently study the dynamics of the initial stages of folding by placing the pair near the chain end. It is interesting to note that similar behavior is observed in protein folding, in the sense that there are nucleation centers where secondary structures are first formed. It is also noteworthy that for large R_F FRET does not last until the completion of the folding process. For the chosen set of parameters, the maximum FRET time observed is 300τ. On the other hand, for the same polymer chain, the late stage of folding continues for times beyond 450τ (see Figure 4). This leads to

the conclusion that for FRET to be a reliable marker of the polymer folding pathway, one would need to use several donor−acceptor pairs. FRET may also be able to differentiate between different collapsed states, like rod and toroid. Because there is no unique ground state for homopolymers, rods might gives rise to a slow decay in $S_P(t)$, followed by an initial fast one, relative amplitudes depending on the fractions of rods where the two ends are close to each other. Toroid should always give a fast decay. Further work in this direction is under progress.

Acknowledgment. It is pleasure to thank Professor Peter J. Rossky for fruitful discussions. The financial support from CSIR, New Delhi, India and DST, India is gratefully acknowledged. G.S. thanks CSIR for a research fellowship. A.Y. would like to acknowledge SSCU for the hospitality during his stay and the National Science Foundation for support (through Grant No. CHE-9732604).

References and Notes

(1) Karplus, M.; Weaver, D. L. *Nature* **1976**, *260*, 404.

(2) Shaknovich, E. I.; Finkelstein, A. V. *Biopolymers* **1989**, *28*, 1667.

(3) Bryngelson, J. D.; Wolynes, P. G. *J. Phys. Chem.* **1989**, *93*, 6902.

(4) Hu, Y.; Fleming, G. R.; Freed, K. F.; Perico, A. *Chem. Phys*. **1991**, *158*, 395.

(5) Deniz, A. A.; Dahan, M.; Grunwell, T.; Ha, T.; Faulhaber, A. E.; Chemla, D. S.; Weiss, S.; Schultz, P. G. *Proc. Natl. Acad. Sci. U.S.A.* **1999**, *96*, 3670.

(6) Deniz, A. A.; Laurence, T. A.; Beligere, G. S.; Dahan, M.; Martin, A. B.; Chemla, D. S.; Dawson, P. E.; Schultz, P. G.; Weiss, S. *Proc. Natl. Acad. Sci. U.S.A.* **2000**, *97*, 5179.

(7) Ha, T.; Ting, A. Y.; Liang, J.; Caldwell, W. B.; Deniz, A. A.; Chemla, D. S.; Schultz, P. G.; Weiss, S. *Proc. Natl. Acad. Sci. U.S.A.* **1999**, *96*, 893.

(8) Wallace, M. I.; Ying, L.; Balasubramanian, S.; Klenerman, D. *J. Phys. Chem. B* **2000**, *104*, 11551. Ying, L.; Wallace, M. I.; Balasubramanian, S.; Klenerman, D. *J. Phys. Chem. B* **2000**, *104*, 5171.

(9) Winnik, M. A. *Langmuir* **1997**, *13*, 3103. Yekta, A.; Winnik, M. A.; Farinha, J. P. S.; Martinho, J. M. G. *J. Phys. Chem. A* **1997**, *101*, 1787.

(10) Mizusaki, M.; Morishima, Y.; Winnik, F. M. *Macromolecules* **1999**, *32*, 4317.

(11) Forster, Th. *Ann. Phys. (Leipzig)* **1948**, *2*, 55.

(12) Cantor, C. R.; Pechukas, P. *Proc. Natl. Acad. Sci. U.S.A.* **1971**, *68*, 2099.

(13) Birks, G. B. In *Photophysics of Aromatic Molecules*; Wiley-Interscience: London, U.K., 1970; p. 576.

(14) Stryer, L.; Haugland, R. P. *Proc. Natl. Acad. Sci. U.S.A.* **1967**, *58*, 719.

(15) de Gennes, P. *Scaling Concepts in Polymer Physics*; Cornell University Press: Ithaca, NY, 1979.

(16) Doi, M.; Edwards, S. F. *The Theory of Polymer Dynamics*; Oxford University Press: Oxford, U.K., 1986.

(17) Noguchi, H.; Yoshikawa, K. *J. Chem. Phys.* **2000**, *113*, 854.

(18) Srinivas, G.; Yethiraj, A.; Bagchi, B. *J. Chem. Phys.* Communicated. Srinivas, G.; Bagchi, B. *Chem. Phys. Lett.* **2000**, *328*, 420.